Absence of localization in a class of topological systems

Eduardo V. Castro,[1,2,*] Raphael de Gail,[3] M. Pilar López-Sancho,[3] and María A. H. Vozmediano[3]
[1]*CeFEMA, Instituto Superior Técnico, Universidade de Lisboa, Avenida Rovisco Pais, 1049-001 Lisboa, Portugal*
[2]*Beijing Computational Science Research Center, Beijing 100084, China*
[3]*Instituto de Ciencia de Materiales de Madrid, CSIC, Sor Juana Inés de la Cruz 3, Cantoblanco, E-28049 Madrid, Spain*
(Received 19 February 2016; revised manuscript received 18 April 2016; published 15 June 2016)

Topological matter is a trending topic in condensed matter: From a fundamental point of view, it has introduced new phenomena and tools and, for technological applications, it holds the promise of basic stable quantum computing. Similarly, the physics of localization by disorder, an old paradigm of obvious technological importance in the field, continues to reveal surprises when new properties of matter appear. This work deals with the localization behavior of electronic systems based on partite lattices, with special attention to the role of topology. We find an unexpected result from the point of view of localization properties: A robust topological metallic state characterized by a nonquantized Hall conductivity arises from strong disorder in topological systems based on bipartite lattices. The key issue is the nature of the disorder realization: selective disorder in only one sublattice. The generality of the result is based on the partite nature of most recent two-dimensional materials such as graphene or transition-metal dichalcogenides, and the possibility of the physical realization of the particular disorder demonstrated in Ugeda *et al.* [M. M. Ugeda *et al.*, Phys. Rev. Lett. **104**, 096804 (2010)] and Zhao *et al.* [L. Zhao *et al.*, Science **333**, 999 (2011)].

DOI: 10.1103/PhysRevB.93.245414

I. INTRODUCTION

After the seminal work of Anderson [1], it was understood that in a noninteracting two-dimensional electron system at zero temperature in spatial dimension $D \leqslant 2$ and in the thermodynamic limit, the electronic wave function will be localized by disorder. In more realistic situations, the scaling theory of localization allowed a classification of the localization behavior of materials into universality classes set by symmetry and space dimensionality [2,3] based on the Altland-Zirnbauer sets of random matrices [4]. The advent of topological insulators [5–7] provided a new class of delocalized states, the edge states, robust under disorder provided some discrete symmetries were preserved. The symmetry classes were then adapted to include the topological features and a "tenfold way" classification was set [8,9].

Centering the attention on the three nonchiral symmetry classes of the original Wigner-Dyson classification in two dimensions, we expect the following situation: All states will be localized in the orthogonal class AI (time-reversal symmetry $\mathcal{T}$ with $\mathcal{T}^2 = 1$ preserved), and a mobility edge [10], i.e., a well-defined energy separating a region of extended states from the localized states, is expected in the symplectic class AII (time-reversal symmetry with $\mathcal{T}^2 = -1$ preserved). Finally, in the unitary class A ($\mathcal{T}$ broken), extended states can remain at particular energies but no mobility edge will be present. Only classes A and AII support topological indices. The prototypical examples in class A are systems showing the integer quantum Hall effect (IQHE) and anomalous quantum Hall systems, the latter exemplified by the Haldane model [11]. Spin Hall systems [12,13] belong to class AII.

The interplay of topology and localization was first analyzed in the context of the robustness under disorder of the Hall conductivity quantization in the IQHE [14–17]. This is an example of a Chern insulator that belongs to symmetry class A (all discrete symmetries are broken) in the standard classification. The mechanism for localization in both topological classes A and AII is referred to as "levitation and annihilation" [18]. For moderate disorder, the states in the edges of the conduction and valence bands start to localize. As disorder increases, the gap is totally populated by localized states and the extended states carrying the Chern number shift towards one another and annihilate, leading to the topological phase transition. The difference between the two classes is that while in the symplectic class AII a finite region of extended states with a well-defined mobility edge remains until the transition takes place, there is no mobility edge in the unitary class A systems. The extended states carrying the Chern number are located at particular single energies.

We use the Haldane model [11] as a typical example of a class A system based on a bipartite lattice. As it is known, depending on the parameter values, the model can represent a Chern or a trivial insulator. The main result of this work is the finding of an extended region of delocalized states with a well-defined mobility edge that emerges for strong disorder in class A systems when disorder is selectively distributed in only one sublattice. This is a surprising result and is against the traditional view since no mobility edge should be expected in this class. Moreover, the final metallic state is an anomalous Hall metal even in the case when the clean starting system is a topologically trivial insulator with $\mathcal{T}$ broken. Hence our result implies that the standard classification has to be complemented.

In addition to its fundamental interest, the physics of this work can be relevant to understanding the effects of disorder in actual material systems. Many of the two-dimensional (2D) materials relevant for technological or fundamental physics are based on bipartite lattices. The most prominent examples, i.e., graphene and its siblings silicene, germanene, or stanene, as well as boron nitride or transition-metal dichalcogenides MX_2 (M = Mo, W and X = S, Se), are based on the honeycomb

*eduardo.castro@tecnico.ulisboa.pt

lattice [19]. Topological materials are based on lattices having at least two atoms per unit cell. Most of them are also defined on partite lattices. Experiments done in graphene show the experimental possibility of inducing disorder selectively in one sublattice only [20], and how certain dopants sit preferentially in only one sublattice [21].

II. MODEL AND METHODS

We use the Haldane model [11] as a generic example of a Chern topological insulator. The Haldane model tight-binding Hamiltonian can be written as

$$H = -t \sum_{\langle i,j \rangle} c_i^\dagger c_j - t_2 \sum_{\langle\langle i,j \rangle\rangle} e^{-i\phi_{ij}} c_i^\dagger c_j + M \sum_i \eta_i c_i^\dagger c_i, \quad (1)$$

where $c_i = A, B$ are defined in the two triangular sublattices that form the honeycomb lattice. The first term t represents a standard real nearest-neighbor hopping that links the two triangular sublattices. The next term represents a complex next-nearest-neighbor hopping $t_2 e^{-i\phi_{ij}}$ acting within each triangular sublattice with a phase ϕ_{ij} that has opposite signs $\phi_{ij} = \pm\phi$ in the two sublattices. This term breaks time-reversal symmetry and opens a nontrivial topological gap at the Dirac points. The last term represents a staggered potential ($\eta_i = \pm 1$). It breaks inversion symmetry and opens a trivial gap at the Dirac points. The topological transition occurs at $|M| = 3\sqrt{3} t_2 \sin\phi$, as shown in Fig. 1. Most of our calculations have been done for the simplest case $\phi = \pi/2$ and a typical value $t_2 = 0.1t$. The trivial mass M has been set to zero, except when analyzing the topologically trivial case. A physical realization of the model with optical lattices has been presented in [22] (see also [23]).

Potential (Anderson) disorder is implemented by adding to the Hamiltonian the term $\sum_{i \in A,B} \varepsilon_i c_i^\dagger c_i$, with a uniform distribution of random local energies, $\varepsilon_i \in [-W/2, W/2]$. We will discuss two cases: disorder equally or selectively distributed among the two sublattices. For selective disorder, the sum runs only over one sublattice.

The Haldane model belongs to symmetry class A where the different topological phases can be characterized by a $\mathbb{Z}$-topological number, the Chern number ν (see Fig. 1). In the clean insulating system, it can be computed from the single-particle Bloch states $u_n(\mathbf{k})$ as

$$\nu_n = \frac{1}{2\pi} \int_S \Omega_z^n(k) dS, \quad (2)$$

where the integral is over the first Brillouin zone S and $\Omega_z^n(k)$ is the z component of the Berry curvature, $\Omega^n(\mathbf{k}) = \nabla_k \wedge A_n(\mathbf{k})$, defined from the Berry connection, $\mathcal{A}_n(\mathbf{k}) = \langle u_n(\mathbf{k}) | -i\nabla_{\mathbf{k}} | u_n(\mathbf{k}) \rangle$. The nontrivial topology of metallic states (anomalous Hall systems) is associated with a finite, non-quantized Hall conductivity that can be computed using a Kubo formula. The main technical difficulty in addressing disordered systems is the breakdown of translational symmetry, which prevents working directly in momentum space. The subject being very old, many numerical and analytical tools have been worked out to deal with this oddity. Topological systems share the same problem, as most topological indices are naturally defined in k space. We have used a numerical recipe based on the Kubo formula to compute the Hall conductivity in the disordered tight-binding model similar to that described in [24].

The localization behavior of the system has been explored with standard tools: level spacing statistics and inverse participation ratio (IPR) [9]. A transfer matrix method [25] has also been used to compute the localization length and confirm the presence of a mobility edge.

III. WARMING UP: DISORDER EQUALLY DISTRIBUTED IN BOTH SUBLATTICES

We first present the case of Anderson disorder equally distributed in the two sublattices which shows the standard behavior of class A systems: extended states carrying the topological index remain at singular energies, approach each other as disorder increases (levitation), and merge (annihilation of the topological index). Figure 2 shows the spectrum for the Haldane model with Anderson disorder equally distributed over the two sublattices for a disorder strength $W = 3t$. The black dots at a given height correspond to the set of

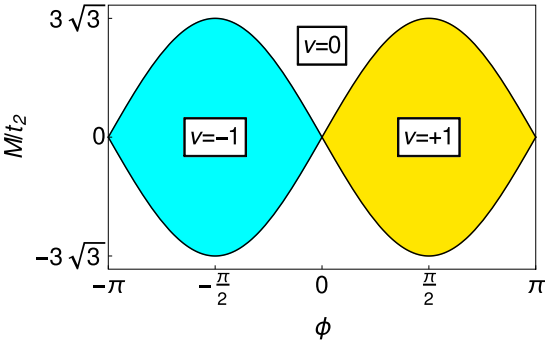

FIG. 1. Phase diagram of the Haldane model as a function of the parameters M and ϕ with $|t_2/t| < 1/3$. The condition $|M| = 3\sqrt{3} t_2 \sin\phi$ sets the boundary between a trivial (Chern number $\nu = 0$) and a topological ($\nu = \pm 1$) insulator.

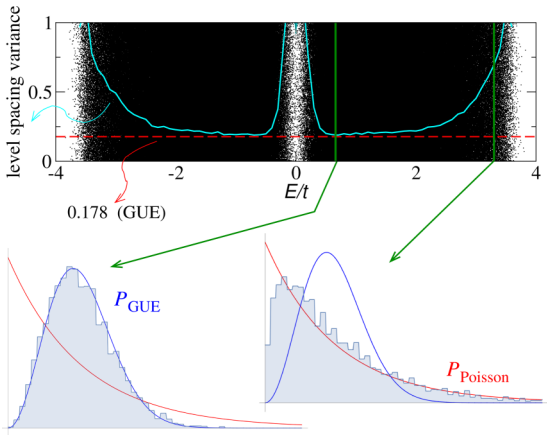

FIG. 2. Level statistics analysis for the Haldane model with Anderson disorder $W = 3t$ equally distributed over the two sublattices. States are localized (Poisson distribution, P_{Poisson}) all along the energy range. Extended states (GUE statistics, P_{GUE}) are found at the two singular energies where the level spacing variance approaches 0.178. This result agrees with the analysis done in Ref. [27].

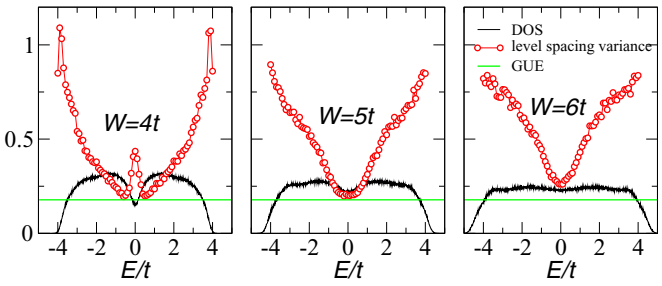

FIG. 3. Localization transition studied through level statistics for the Haldane model with Anderson disorder equally distributed over the two sublattices. The horizontal green line marks the GUE variance. The two extended states present at $W = 3t$ merge around $W = 5t$ and annihilate as disorder increases. All states become localized for $W > W_c \sim 5t$. The average DOS is also shown.

eigenenergies for a given disorder realization in a finite lattice with size $d = 30$. We have performed 1000 disorder realizations, shown at slightly different heights. Superimposed to the spectrum we show the level spacing variance as a function of energy. The variance of the level spacing variation contains information on the localization of the states at a given energy region (details can be found in Appendix B). The statistics of the Gaussian unitary ensemble (GUE) is expected only for extended states [26], while localized states follow the Poisson distribution. It is clear that there are two extended states, one below the gap and another one above, where the variance clearly approaches the GUE variance 0.178. These results are in perfect agreement with those presented in Ref. [27]. In Fig. 3, we show the level statistics variance and the density of states (DOS) for three different disorder strengths: $W = 4t,5t,6t$. Levitation and annihilation is clearly operative, and the critical disorder for localization is in good agreement with that obtained in Ref. [28] for the topological transition, $4t < W_c < 5t$.

IV. MAIN RESULTS: DISORDER SELECTIVELY DISTRIBUTED IN ONLY ONE SUBLATTICE AND ANOMALOUS HALL METAL

The unexpected result obtained is that for selectively distributed disorder in only one sublattice, the class A systems with nontrivial topology end up in a robust metallic state where the extended states are separated from the localized states by a well-defined mobility edge. This result is unconventional in two ways: First the absence of localization for very strong disorder is unusual for any system. Second, in the standard classification, class A systems do not support a mobility edge. Figure 4 shows a level spacing statistic analysis of the Haldane model in the topological phase for increasing disorder strength. In the figure, we see the level spacing variance as a function of energy and the distribution of level spacings associated with two characteristic energies in the spectrum: one at higher energies (blue line), where states start to localize first when disorder is introduced, and one at lower energies, close to the middle of the spectrum (green line) where extended states are expected to persist up to higher disorder strength. The red dotted horizontal line marks the variance of the GUE associated with the presence of extended states. We see that as

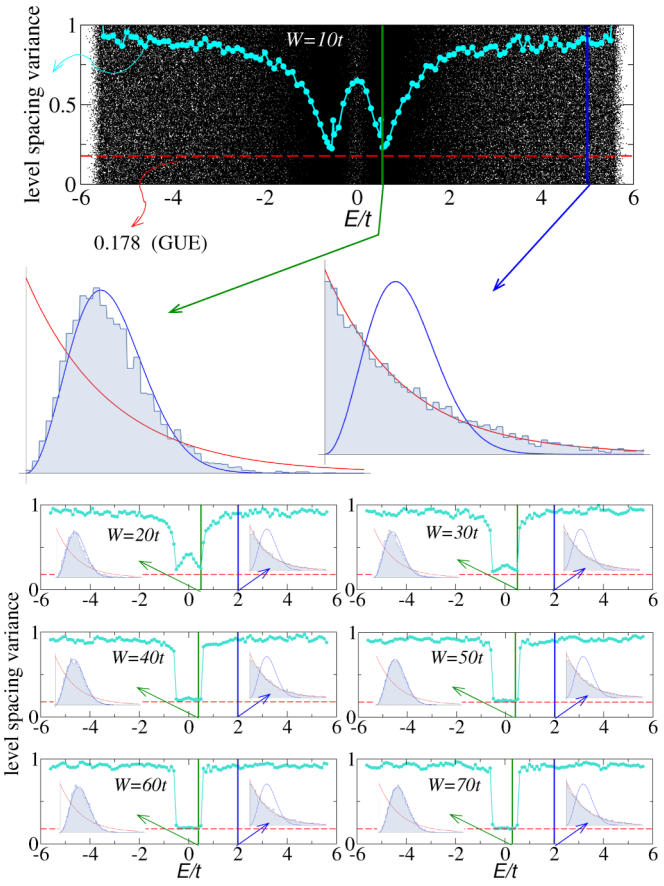

FIG. 4. Level statistics analysis for the Haldane model with Anderson disorder selectively distributed over one sublattice. The red dotted horizontal line marks the variance of the GUE associated with the presence of extended states. As disorder increases, the singular energies where extended states were located at moderate disorder strength $W/t = 10$–30 evolve to a full extended region of delocalized states with a well-defined mobility edge.

disorder increases, the singular energies where extended states were located at moderate disorder strength $W/t = 10$–30 evolve to a full extended region of delocalized states with a well-defined mobility edge. Figure 5 shows that the extended region of delocalized states is a robust feature that persists up to a disorder strength of $W = 200t$. We have also set up a calculation of the localization length via a transfer matrix method to confirm the presence of the mobility edge (see Appendix A).

The topological nature of the metallic state is reflected in the calculation of the Hall conductivity shown in Fig. 6. In our previous publication [28], we showed that the Chern insulator suffered a topological transition to a state with nonquantized Chern number at a critical disorder strength around $W_c \sim 50t$. What we see here is the further evolution to an anomalous Hall metal when disorder is further increased and the metallic state is well established. The panels in Fig. 6 show that the Hall conductivity stays finite in the metallic region for $W > W_c$. The different curves correspond to different sizes of the system. We see that for increasing system sizes, σ_{xy} is not decreasing which proves that we are not dealing with a finite-size effect. Despite the large numerical error bars, a finite conductivity can

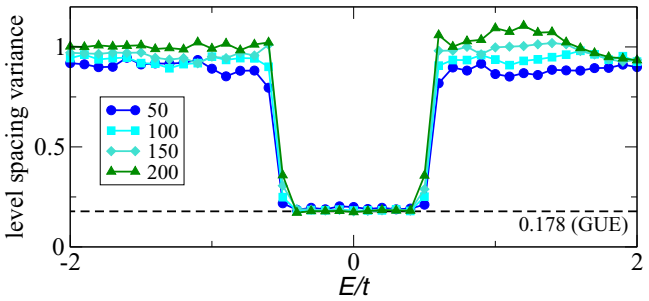

FIG. 5. Level spacing variance for increasing disorder strengths W/t in the selectively distributed disorder case. The middle region has the same variance as that of GUE and corresponds to extended states. Even though the transition is becoming sharper, the region is not shrinking. This is clear evidence for the existence of an extended region of delocalized states. A mobility edge in the center of the band has emerged from the singular, isolated energies by increasing disorder.

be granted. The same analysis done for the Haldane model in the trivial phase shows that the final state is also an anomalous Hall metal.

V. UNDERSTANDING WHAT IS GOING ON: SIDE QUESTIONS

This work brings up a number of questions. We have addressed some of them with the help of the additional calculations detailed in the appendices, but others remain open.

Disordered systems are classified according to their discrete symmetries (time reversal, inversion, and particle hole) and their topology. From the examples discussed in the appendices, it is clear that the main role in the absence of localization is played by the nontrivial topology of the conduction and valence bands of the clean system. Particle-hole symmetry does not seem to play a role.

We have found that when the bands of the clean system have nontrivial Berry curvature, the final state analyzed in class A is a $\mathcal{T}$ broken disordered metal with finite Hall conductivity (irrespective of the global "Chern number" of the initial state). A topologically nontrivial system in class AII is the model of Kane and Mele for the spin Hall insulator [12]. Since it is

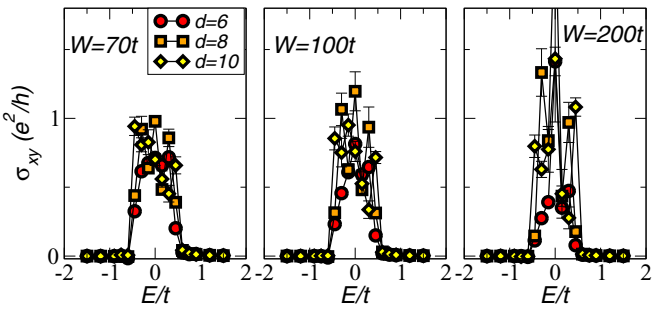

FIG. 6. Hall conductivity of the resulting metallic state emerging from the Chern insulator for disorder strengths above the critical value for the topological transition. The conductivity is not quantized and depends on the chemical potential. Despite the big numerical bars, a finite nonzero value can be granted.

made of two copies of the Haldane model with opposite Chern numbers for the two spin species and the disorder does not mix the spins, the final state will also be metallic with nontrivial spin Hall conductivity. This shows that time-reversal symmetry is not playing a crucial role in the absence of localization.

It is tempting to think that the obtained metallic state belongs to the clean triangular sublattice only. Its topological nature, though, proves that this is not so, since the anomalous Hall effect is due to the interband matrix elements of the current operator [29]. The analysis of the partial IPR (see Appendix B) shows that the extended states found in the extreme disorder case have a nonzero (although suppressed by orders of magnitude with respect to the clean sublattice) extended weight in the disordered sublattice. This can be understood starting from the limit where the two sublattices are not connected ($t = 0$). The parameter t connects the two T broken triangular sublattices, one with all states localized and the other one with all states extended. Treating t as a perturbation, the perturbed states will be a superposition of extended and localized states, which is still an extended state.

The metallicity of the final state seems to be at odds with the nonlinear σ model results [9,30], so it would be very interesting to implement the selective disorder case in this approach.

A similar metallic phase has also been described recently in [31,32] at intermediate disorder strength, but it goes away by increasing disorder in these examples. A possible explanation for the intermediate metal phase in [31] is the existence of a pseudo-time-reversal symmetry that makes the system approximately symplectic.

The physics described in this work can be realized in topological materials based on other more complicated partite lattices [33]. The results presented in this work are conceptually important and can be useful to interpret experiments in the honeycomb lattice doped with adatoms sitting preferentially in one sublattice, as described in Ref. [21]. Artificial [34] or optical [22] lattices are other possibilities to realize this physics.

ACKNOWLEDGMENTS

We gratefully acknowledge useful conversations with Alberto Cortijo, Belén Valenzuela, Fernando de Juan, Adolfo G. Grushin, and J. A. Vergés. E.C. acknowledges the financial support of FCT-Portugal through Grant No. EXPL/FIS-NAN/1728/2013. This research was supported in part by the Spanish MECD Grant No. FIS2014-57432-P, the European Union structural funds, and the Comunidad de Madrid MAD2D-CM Program (S2013/MIT-3007), as well as the European Union Seventh Framework Programme under Grant Agreement No. 604391 Graphene Flagship FPA2012-32828.

APPENDIX A: LOCALIZATION LENGTH VIA A TRANSFER MATRIX METHOD TO CONFIRM THE PRESENCE OF THE MOBILITY EDGE

Our main result is the finding that for Anderson disorder selectively distributed in only one sublattice, the metallic state is robust no matter how large the disorder. We have set up a calculation of the localization length λ_M transfer matrix method as used in Ref. [18]. The results for selective disorder are shown in Fig. 7. It is apparent that a region of extended states, for which the renormalized localization length $\lambda_M/M \equiv$

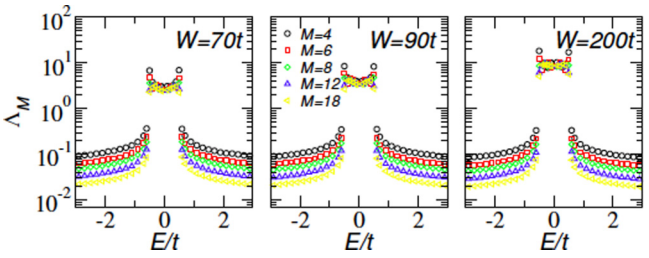

FIG. 7. Renormalized localization length Λ_M as a function of the (linear) system size (M) calculated for various disorder strengths W_i by the transfer matrix method.

$\Lambda_M = \texttt{const}$ (typical of a critical behavior), shows up around $E = 0$. This proves the existence of a mobility edge.

APPENDIX B: UNDERSTANDING THE NATURE OF EXTENDED STATES IN THE ANOMALOUS HALL PHASE

It might appear at first sight that the transition that we are describing occurs between a topological insulator based on the honeycomb lattice (Haldane model) to a pure triangular lattice with imaginary hoppings (metallic). In order to investigate the properties of the extended wave function, we have performed calculations of the partial IPR in the disordered sublattice (partial IPR is like conventional IPR, but the lattice summation is over a single sublattice). We expected to find a critical disorder W_c^{sub} above which all states become localized in that sublattice. This critical disorder should coincide with the value when the Chern number ceases to be quantized. The results in Fig. 8 indicate that delocalized states are also present on the disordered sublattice at extremely large disorder. We have seen that extended states have a finite, extended weight in the disordered sublattice. This is an essential ingredient because if states were only extended in the nondisordered sublattice, the physics would be that of a single band. Since the anomalous Hall effect is due to the interband matrix elements of the current operator, no anomalous Hall response could be found. It is appealing to interpret these extended states starting from the limit where the two sublattices are not connected, when $t = 0$. In this case, we have a T broken triangular lattice where all states are localized, i.e., the disordered sublattice, and a T broken triangular lattice where all states are extended, i.e., the clean sublattice. If one then assumes that connecting the two sublattices perturbatively with t does not break the extended character of the states in the clean sublattice, we then see that the new perturbed states would be superpositions of localized states with extended states. A state which is a superposition of an extended state with a localized state is still an extended state. This explains why we observe extended states in the full energy region where the clean sublattice develops its band. Moreover, it also explains why the perturbed states look like extended states in the disordered sublattice also. This happens because the perturbation will mix the states closest in energy, and for localized states those are the furthest apart in space. A very simple relation between the energy difference ΔE between localized states, their spatial distance R, and the DOS $\rho(E)$ at the typical energy E where these states occur can be derived [25],

$$\Delta E \sim [R^d \rho(E)]^{-1}, \tag{B1}$$

where d is the spatial dimension. The smallest ΔE results in the largest R. In deriving the last expression, it is assumed that localized states are homogeneously distributed. A superposition of those closest in energy would then have a finite weight at points very far apart on the lattice and, like a tight-binding description of an electron in a solid, the respective wave function would be extended. The reasoning

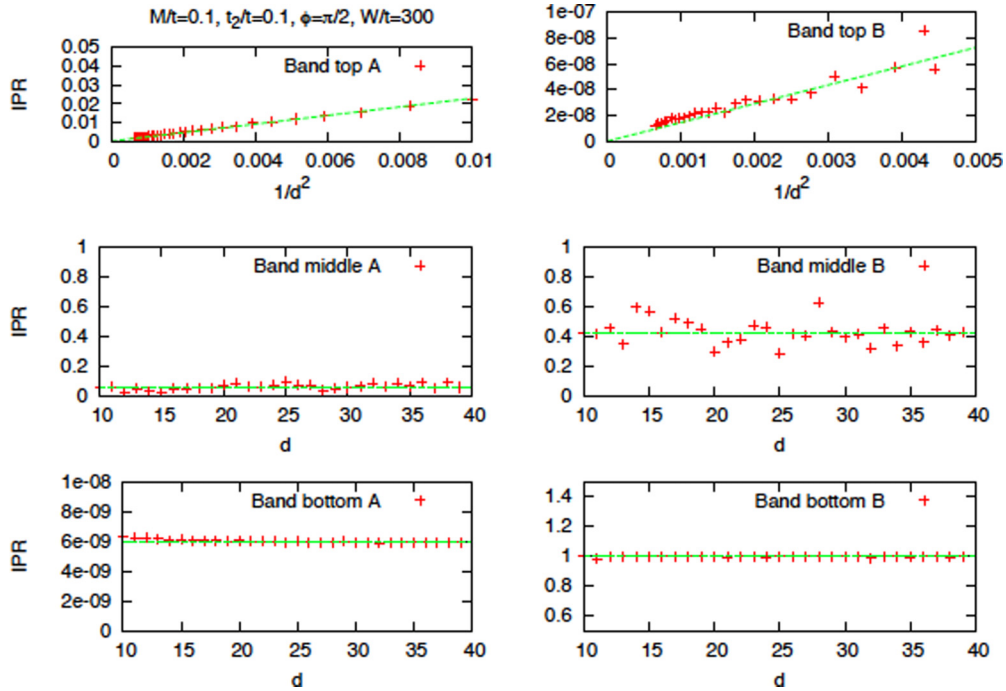

FIG. 8. Partial IPR for strong ($W > 300$) disorder selectively located in sublattice B. Electrons in this sublattice are also delocalized even though the IPR is very small.

above is limited by the assumption that extended states in the clean sublattice remain extended even for finite t when we connect the two sublattices. If the system was T invariant, with real t_2, we know that the assumption would not hold, as there are no extended states in that case. We may then anticipate that breaking T, or maybe having finite Berry curvature, plays a key role here, but at the moment we lack an explanation for why the extended states in the clean sublattice remain extended.

APPENDIX C: ROLE OF TOPOLOGY IN THE CASE OF SELECTIVE DISORDER

In order to ascertain the role played by the nontrivial band topology on the localization properties of the class A systems, we have analyzed the localization properties of a pure triangular lattice with imaginary (Haldane) hoppings (the band has no Berry curvature). The Haldane model in the trivial phase (the bands have a nonhomogeneous Berry curvature, but the Chern number cancels when the chemical potential lies in the gap) gives rise to a topological metal as in the topological case.

In Fig. 9, we show the level spacing variance for Anderson disorder with strength $W/t = 0.5, 1, 10$ in the triangular lattice with complex hoppings $t_2 = 0.1t$. It is clear that except for the lowest disorder simulated here, where finite-size effects might be important, all states are localized.

This result reinforces the idea that it is the presence of nontrivial Berry curvature in the valence and conduction bands that plays a role in the absence of localization.

APPENDIX D: ROLE OF TIME-REVERSAL SYMMETRY

AI systems on bipartite lattices have time-reversal symmetry. The next question we have asked is: Does a class AI system with intrasublattice hopping display a metallic phase for large enough selective disorder? The Haldane model with real NNN hoppings belongs to this class. Figure 10 shows the level spacing statistics with $t_2 = 0.1t$ and $M = t$. There are no extended states. Note that even for $W = 300t$, the level spacing variance is always different from GUE. This analysis clarifies several things. First that the selective disorder analyzed through the work does act as standard Anderson disorder since the system analyzed undergoes localization

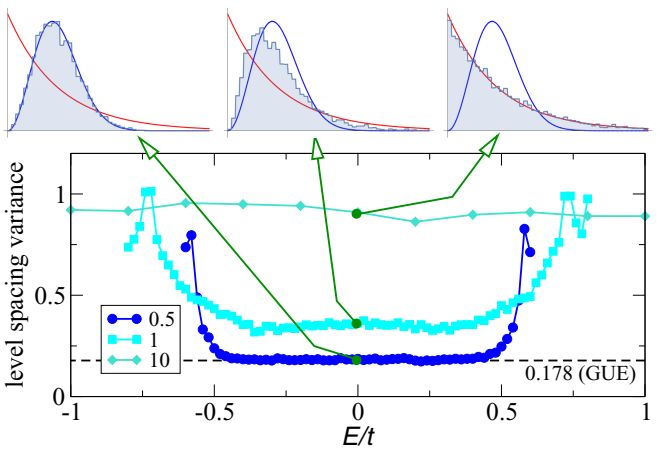

FIG. 9. Level spacing variance for Anderson disorder with strength $W = t = 0:5; 1; 10$ in the triangular lattice with complex hoppings $t_2 = 0.1t$.

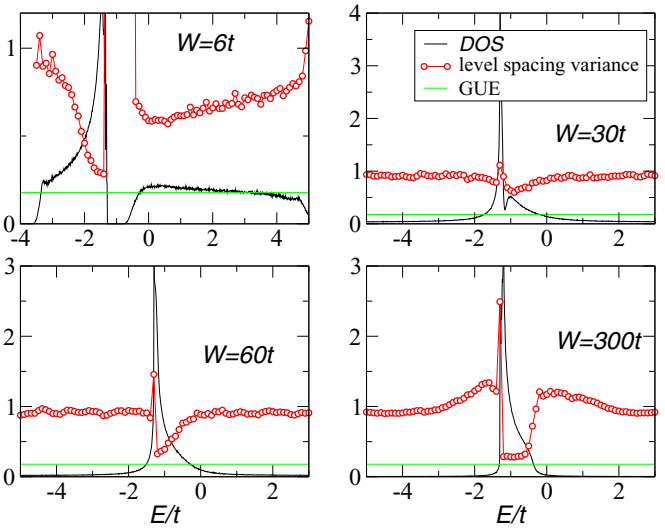

FIG. 10. Level space variance for the Haldane model with real NNN hoppings. The system belongs to class AI: Time-reversal symmetry is preserved and inversion is broken. The system undergoes standard Anderson localization.

even though one sublattice remains perfect. Since the model is topologically trivial, we cannot conclude anything on the role of time-reversal symmetry. This result reinforces the correlation between the absence of localization and nontrivial topology. That time-reversal symmetry is not playing a major role in the absence of localization is indicated by the analysis of the Kane-Mele model discussed in the main text.

APPENDIX E: ROLE OF PARTICLE-HOLE SYMMETRY: CLASS D VERSUS CLASS A

For simplicity, a purely imaginary value of the next-nearest-neighbor hopping parameter has been used through the work ($\phi = \pi/2$). This choice induces an accidental particle-hole symmetry in the system and technically it belongs to class D. For this class, it is known that a metallic phase shows up with increasing disorder. Anderson disorder breaks this symmetry, but on average it is restored. In order to ascertain that our results refer to class A systems, we have performed a calculation of

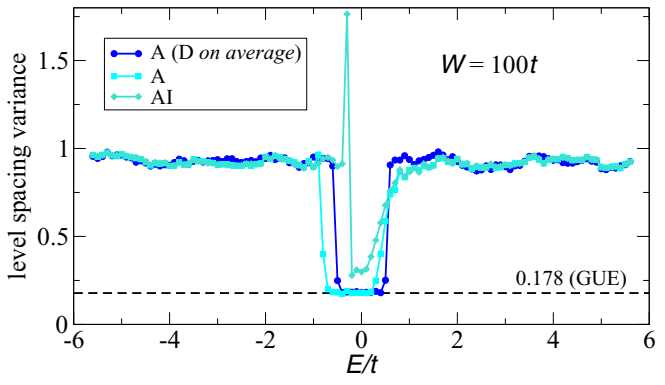

FIG. 11. Level spacing variance for Anderson disorder on a single sublattice in three different systems based on the Haldane model: NNN with a real part. The system is in class A and has no particle-hole symmetry.

the level spacing variance for the model with NNN having a finite real part. In Fig. 11, we show the level spacing variance for Anderson disorder on a single sublattice in three different systems: one with purely imaginary NNN hoppings (Haldane), which belongs to the symmetry class D due to particle-hole symmetry (Anderson disorder breaks it, rendering the system class A, although on average the symmetry is restored); another one with complex NNN hoppings, where the real part breaks particle-hole symmetry and the system is in class A even in the absence of disorder (we used $t_2 = 0.1t + i0.1t$); and finally one with NNN hoppings purely real, thus preserving time-reversal symmetry, as required in symmetry class AI. It is apparent that the only difference between the first (class D on average) and second (class A) cases is a small shift of the region of extended states. This shift is a consequence of the breaking of particle-hole symmetry. For the system in class AI, there are no extended states, as expected, although the presence of a Dirac point at $E = -3(\mathrm{Re}t_2) = -0.3t$ still makes the level spacing variance unconventional, even for such strong disorder. The conclusion is that the physics we are unveiling here is characteristic of class A, *where no mobility edge is expected*, and not from class D.

[1] P. W. Anderson, Absence of diffusion in certain random lattices, Phys. Rev. **109**, 1492 (1958).

[2] E. Abrahams, P. W. Anderson, D. C. Licciardello, and T. V. Ramakrishnan, Scaling Theory of Localization: Absence of Quantum Diffusion in Two Dimensions, Phys. Rev. Lett. **42**, 673 (1979).

[3] P. W. Anderson, D. J. Thouless, E. Abrahams, and D. S. Fisher, New method for a scaling theory of localization, Phys. Rev. B **22**, 3519 (1980).

[4] A. Altland and M. R. Zirnbauer, Nonstandard symmetry classes in mesoscopic normal-superconducting hybrid structures, Phys. Rev. B **55**, 1142 (1997).

[5] B. A. Bernevig, T. L. Hughes, and S. Zhang, Quantum spin hall effect and topological phase transition in hgte quantum wells, Science **314**, 1757 (2006).

[6] M. Z. Hasan and C. L. Kane, Topological insulators, Rev. Mod. Phys. **82**, 3045 (2010).

[7] X. Qi and S. Zhang, Topological insulators and superconductors, Rev. Mod. Phys. **83**, 1057 (2011).

[8] A. P. Schnyder, S. Ryu, A. Furusaki, and A. W. W. Ludwig, Classification of topological insulators and superconductors in three spatial dimensions, Phys. Rev. B **78**, 195125 (2008).

[9] F. Evers and A. D. Mirlin, Anderson transitions, Rev. Mod. Phys. **80**, 1355 (2008).

[10] P. A. Lee and T. V. Ramakrishnan, Disordered electronic systems, Rev. Mod. Phys. **57**, 287 (1985).

[11] F. D. M. Haldane, Model for a Quantum Hall Effect without Landau Levels: Condensed-Matter Realization of the Parity Anomaly, Phys. Rev. Lett. **61**, 2015 (1988).

[12] C. L. Kane and E. J. Mele, Quantum Spin Hall Effect in Graphene, Phys, Rev. Lett. **95**, 226801 (2005).

[13] C. L. Kane and E. J. Mele, Z2 Topological Order and the Quantum Spin Hall Effect, Phys, Rev. Lett. **95**, 146802 (2005).

[14] A. M. M. Pruisken, The integral quantum hall effect: Shortcomings of conventional localization theory, Nucl. Phys. B **295**, 653 (1988).

[15] A. M. M. Pruisken, Universal Singularities in the Integral Quantum Hall Effect, Phys. Rev. Lett. **61**, 1297 (1988).

[16] J. T. Chalker and P. D. Coddington, Percolation, quantum tunneling and the integer hall effect, J. Phys. C: Solid State Phys. **21**, 2665 (1988).

[17] A. W. W. Ludwig, M. P. A. Fisher, R. Shankar, and G. Grinstein, Integer quantum Hall transition: An alternative approach and exact results, Phys. Rev. B **50**, 7526 (1994).

[18] M. Onoda, Y. Avishai, and N. Nagaosa, Localization in a Quantum Spin Hall System, Phys. Rev. Lett. **98**, 076802 (2007).

[19] E. Gibney, The super materials that could trump graphene, Nature (London) **522**, 274 (2012).

[20] M. M. Ugeda, I. Brihuega, F. Guinea, and J. M. Gómez-Rodríguez, Missing Atom as a Source of Carbon Magnetism, Phys. Rev. Lett. **104**, 096804 (2010).

[21] L. Zhao *et al.*, Visualizing individual nitrogen dopants in monolayer graphene, Science **333**, 999 (2011).

[22] G. Jotzu *et al.*, Experimental realization of the topological haldane model with ultracold fermions, Nature (London) **515**, 237 (2014).

[23] A. R. Wright, Realising Haldane's vision for a Chern insulator in buckled lattices, Sci. Rep. **3**, 2736 (2013).

[24] A. Crepieux and P. Bruno, Theory of the anomalous hall effect from the kubo formula and the dirac equation, Phys. Rev. B **64**, 014416 (2001).

[25] B. Kramer and A. MacKinnon, Localization: Theory and experiment, Rep. Prog. Phys. **56**, 1469 (1993).

[26] R. J. Elliott, J. A. Krumhansl, and P. L. Leath, The theory and properties of randomly disordered crystals and related physical systems, Rev. Mod. Phys. **46**, 465 (1974).

[27] E. Prodan, Disordered topological insulators: A non-commutative geometry perspective, J. Phys. A: Math. Theor. **44**, 113001 (2011).

[28] E. V. Castro, M. P. López-Sancho, and M. A. H. Vozmediano, Anderson localization and topological transition in chern insulators, Phys. Rev. B **92**, 085410 (2015).

[29] R. Karplus and J. M. Luttinger, Hall effect in ferromagnetics, Phys. Rev. **95**, 1154 (1954).

[30] T. Morimoto, A. Furusaki, and C. Mudry, Anderson localization and the topology of classifying spaces, Phys. Rev. B **91**, 235111 (2015).

[31] C.-Z. Chen, H. Liu, H. Jiang, Q.-F. Sun, Z. Wang, and X. C. Xie, Tunable anderson metal-insulator transition in quantum spin-hall insulators, Phys. Rev. B **91**, 214202 (2015).

[32] Z. Qiao *et al.*, Anderson localization from Berry-curvature interchange in quantum anomalous Hall system, arxiv:1601.07367.

[33] G. Xu, B. Lian, and S. C. Zhang, Intrinsic Quantum Anomalous Hall Effect in the Kagome Lattice $Cs_2LiMn_3F_{12}$, Phys. Rev. Lett. **115**, 186802 (2015).

[34] K. K. Gomes, W. Mar, W. Ko, F. Guinea and H. C. Manoharan, Designer Dirac Fermions and topological phases in molecular graphene, Nature (London) **483**, 306 (2012).